VISCID/INVISCID INTERACTION ANALYSIS OF THRUST AUGMENTING EJECTORS

P. M. Bevilaqua and A. D. DeJoode
Rockwell International
Columbus Aircraft Division

- Abstract -

A method has been developed for calculating the static performance of thrust augmenting ejectors by matching a viscous solution for the flow through the ejector to an inviscid solution for the flow outside the ejector. A two-dimensional analysis utilizing a turbulence kinetic energy model is used to calculate the rate of entrainment by the jets. Vortex panel methods are then used with the requirement that the ejector shroud must be a streamline of the flow induced by the jets to determine the strength of circulation generated around the shroud. In effect, the ejector shroud is considered to be "flying" in the velocity field of the jets. The solution is converged by iterating between the rate of entrainment and the strength of the circulation. This approach offers the advantage of including external influences on the flow through the ejector. Comparisons with data are presented for an ejector having a single central nozzle and Coanda jet on the walls. The accuracy of the matched solution is found to be especially sensitive to the jet flap effect of the flow just downstream of the ejector exit.

INTRODUCTION

Analytic procedures for calculating ejector performance are necessary to guide research and for preliminary design studies. The analytic methods that have been developed to date are based broadly on von Karman's now classical momentum analysis.[1] These methods[2-4] deal only with the flow inside the ejector. The thin shear layer approximations are applied to reduce the governing elliptic equations to a parabolic set, which can be solved by marching through the ejector in the streamwise direction. This approach has been useful in identifying some of the factors that affect the level of augmentation and in predicting the results of particular changes in the ejector geometry. However, since elliptic effects are neglected, these solutions are limited to cases in which the ejector is relatively long and the diffuser angle is small.

The purpose of this paper is to present an ejector analysis not subject to these limitations. The primary elliptic effects are included by iterating between a parabolic solution for the flow through the ejector and an elliptic solution for the flow outside the ejector. This technique is similar to that used in coupling a solution for the displacement thickness of a wing boundary layer to a solution for the external flow. In the next section an outline of ejector theory is presented to introduce the mathematical models used in this analysis. The solution algorithms and the method of iteration are described in the following sections. The predictions of this new model are compared with classical solutions and experimental data in the final section.

PRINCIPLE OF THRUST AUGMENTATION

Although ejector thrust augmentation may seem to utilize a new principle of lift generation, it actually involves no more than a novel application of the familiar circulation theorem of aerodynamic lift. An isolated jet induces an essentially lateral flow of entrained air, as sketched in Figure 1. However,
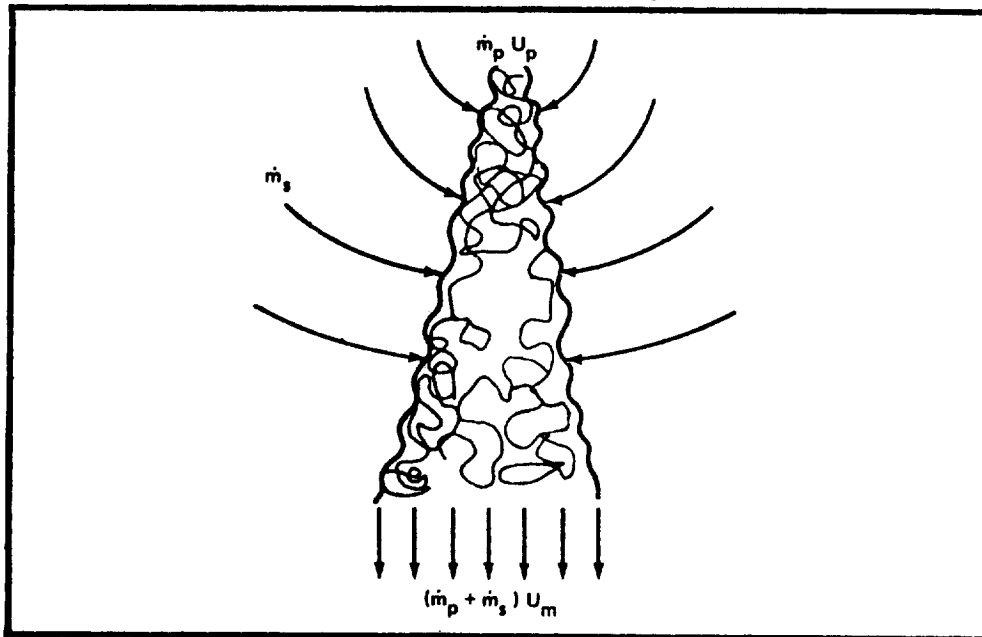

Figure 1. Streamlines of the Flow Induced by a Free Jet.

the distributions of pressure and velocity in the flow outside the ejector
are altered by the shroud. A circulation which redirects the entrained flow
through the ejector is generated around each of the shroud sections, as shown
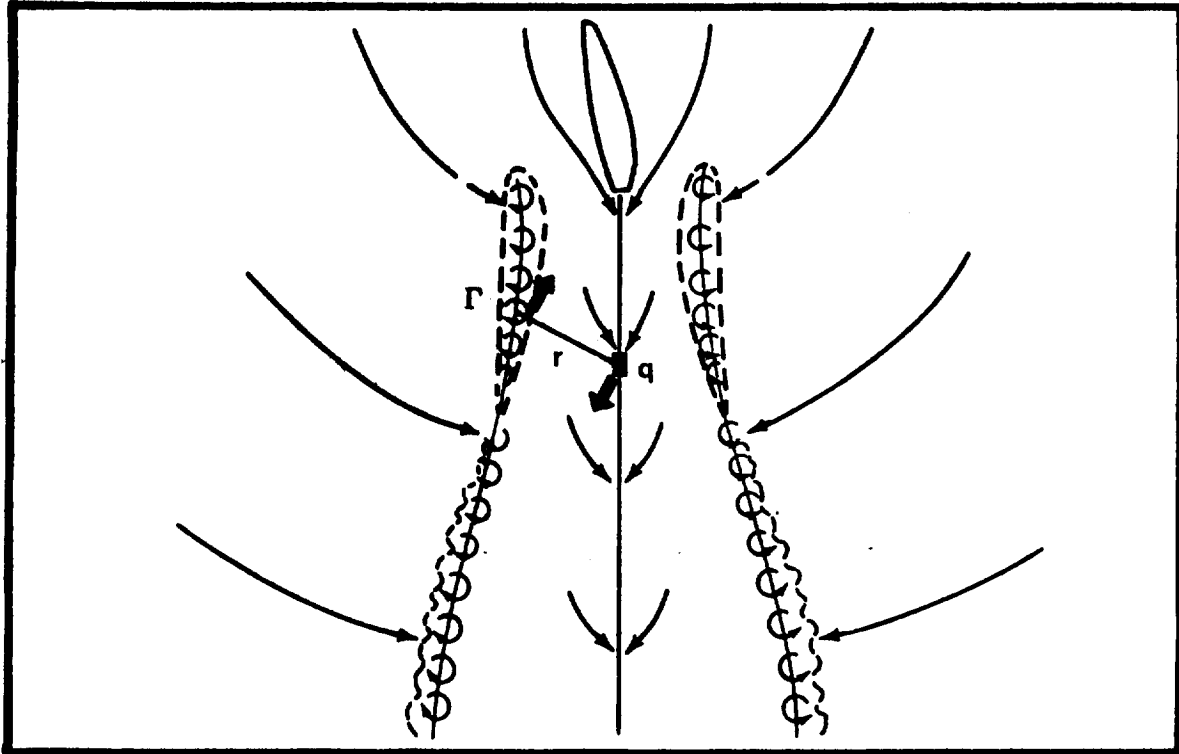in Figure 2. The shroud can therefore be considered to be "flying" in the

Figure 2. A Circulation Redirects the Flow through the Ejector.

velocity field of the flow entrained by the jet, and it experiences a force
analogous to the lift developed on a wing fixed in a moving stream. According
to this lifting surface theory,[5] the thrust augmentation ϕ can be defined as
the ratio of the primary jet thrust T plus the "lift" on the shroud F to the
isentropic thrust of the primary mass:

$$\phi = \frac{T + F}{\dot{m}V} \tag{1}$$

The thrust augmentation results from the fact that the interaction between
the flow induced by the entrainment of the jet and the vorticity bound in the
sections of the shroud generates a pair of equal and opposite forces. The
origin of these forces can be understood by a consideration of the interaction
between a sink of strength Q, which represents a section of the jet, and a
vortex of strength Γ, which represents a segment of the vortex sheet in the
shroud. These singularities are a distance r apart, as shown in Figure 2.

73

At the vortex, the sink induces a velocity of magnitude $Q/2\pi r$, directed along r. The vortex therefore experiences a force $\rho \Gamma Q/2\pi r$, perpendicular to r. At the sink, the vortex induces a velocity of magnitude $\Gamma/2\pi r$, perpendicular to r. The sink therefore experiences a force $\rho Q\Gamma/2\pi r$, also perpendicular to r, but opposite to the force on the vortex. The net effect of the interactions between all the sinks and vortices is a force which increases the thrust of the jet, and an equal but opposite reaction on the shroud.

The force on the shroud can be recognized as the vortex force given by the Kutta-Joukowski theorem for airfoil lift. This force appears in the pressure distribution on the surface of the shroud, primarily as a leading edge suction. The thrust on the jet sinks is conceptually similar to the ram drag that develops on an aircraft inlet. However, it must be remembered that the sink/vortex interaction, as described, only applies to irrotational flows. The flow through the ejector actually includes regions of interacting irrotational and turbulent fluid, subject to lateral straining and streamwise curvature, with variations of temperature and density. In the following section a method of calculating these forces in a real fluid will be developed from the principles outlined in this section.

VISCOUS, INNER SOLUTION

Governing Equations

The entrainment of the jets is calculated from a solution for the turbulent mixing within the ejector. It is possible to calculate the rate of entrainment without solving the complete three-dimensional mixing problem, by taking advantage of the flow geometry. Since there is a primary direction of flow (through the ejector) it is assumed that the thin shear layer approximation can be applied. This approximation means that the gradients of the normal stress are negligible, and the pressure P is constant in each plane normal to the direction of flow. Thus, only shear stresses caused by velocity gradients across the flow are significant. An additional assumption that the fluid density ρ is uniform was also made. Under these assumptions, the equation for the conservation of mass and momentum through the ejector become:

$$\text{Continuity:} \quad \rho \frac{\partial u}{\partial x} = 0 \tag{2}$$

$$\text{Momentum:} \quad \rho u \frac{\partial u}{\partial x} = \frac{\partial \tau}{\partial y} - \frac{dP}{dx} \tag{3}$$

Here, u is the time averaged velocity in the streamwise direction, and τ is the turbulent shear stress. Laminar stresses are assumed to be negligible.

In order to provide accurate calculations of the turbulent stresses in each region of the flow (initial and developed sections of the free jet, inner

74

and outer layers of the wall jet, and the merged region) the two equation turbulence model described by Launder and Spalding[6] was used for turbulence closure. According to the usual eddy viscosity assumption, the turbulent stress is first expressed in terms of a turbulent viscosity μ_t and the velocity gradient in the cross stream direction:

$$\tau = \mu_t \frac{\partial u}{\partial y} \tag{4}$$

The two-equation turbulence model gives the turbulent viscosity in terms of two parameters, for which two differential equations are solved. The expression for turbulent viscosity is:

$$\mu_t = \frac{c_\mu \, \rho \, k^2}{\epsilon} \tag{5}$$

where c_μ is a constant, k is the kinetic energy of turbulence, and ϵ is the rate of its dissipation. In two-dimensional parabolic flows, the governing equations for k and ϵ are:

$$\rho u \frac{\partial k}{\partial x} = \frac{\partial}{\partial y} \left(\frac{\mu_t}{\sigma_k} \frac{\partial k}{\partial y} \right) + G - \rho \epsilon \tag{6}$$

$$\rho u \frac{\partial \epsilon}{\partial x} = \frac{\partial}{\partial y} \left(\frac{\mu_t}{\sigma_\epsilon} \frac{\partial \epsilon}{y} \right) + (c_1 G - c_2 \, \rho \epsilon) \frac{\epsilon}{k} \tag{7}$$

The procedure used to solve the governing equations is very similar to the method devised by Patankar and Spalding.[7] It is basically a finite-difference marching procedure; from known conditions at an upstream cross section, x, the flow field at the downstream cross section, x + Δx, is computed. This marching process is continued until the domain of interest is covered. The initial conditions are determined from the velocities induced in the ejector inlet by the vorticity distribution obtained in the outer solution on the previous iteration. The finite-difference equations are formed by integrating the differential equations over a small control volume surrounding each grid point. The resulting non-linear equations are linearized by using upstream values of the flow variables to evaluate coefficients involving cross stream convection and diffusion. The equations are solved by the use of the tri-diagonal matrix algorithm.

Jet Entrainment Rate

The sink strengths that will represent the effect of the jets in the inviscid calculation are determined from the entrainment of each jet. An entrainment velocity, U_e, is derived from the mass entrained between successive stations, $\dot{m}_e$, according to the definition,

$$U_e = \dot{m}_e / \rho \, \Delta x \tag{8}$$

75

in which Δx is the distance between stations. The entrainment of the central jet is represented by a series of overlapping, triangular sink distributions on the axis of the ejector. Each distribution is identified by the index of its central point, where the strength of the sink is q_j; every panel is the same length, $2s$. The horizontal and vertical components of velocity induced at an arbitrary point $P(x,y)$ by such a distribution are

$$u_s = \frac{q_j}{2\pi}\left\{\frac{y}{s}\left[\tan^{-1}\left(\frac{sy}{x^2 + sx + y^2}\right) + \tan^{-1}\left(\frac{-sy}{x^2 - sx + y^2}\right)\right]\right.$$

$$\left. + \left(\frac{x}{c} + 1\right)\ln\left(\frac{(x+s)^2 + y^2}{x^2 + y^2}\right)^{1/2} + \left(\frac{x}{s} - 1\right)\ln\left(\frac{(x-s)^2 + y^2}{x^2 + y^2}\right)^{1/2}\right\} \quad (9)$$

and

$$v_s = \frac{q_j}{2\pi}\left\{\left(\frac{x}{s} + 1\right)\tan^{-1}\left(\frac{sy}{x^2 + sx + y^2}\right) + \left(\frac{x}{s} - 1\right)\tan^{-1}\left(\frac{-sy}{x^2 - sy + y^2}\right)\right.$$

$$\left. - \frac{y}{s}\left[\ln\left(\frac{(x+s)^2 + y^2}{x^2 + y^2}\right)^{1/2} + \ln\left(\frac{(x-s)^2 + y^2}{x^2 + y^2}\right)^{1/2}\right]\right\} \quad (10)$$

The strengths of the q_j are determined by setting the velocity induced at the midpoint of each triangular distribution equal to the entrainment velocity at that point.

The surface of the ejector shroud is represented by m source panels of different lengths, ℓ_j, and uniform strength, q_j. Because a single sheet of sinks cannot provide the jump in entrainment necessary to model the presence of a wall jet on the inner surface of the shroud only, both the inner and outer surfaces must be represented by source panels. The velocity components induced at an arbitrary point by a uniform source distribution are

$$u_s = \frac{q_j}{2\pi}\ln\left[\frac{(x-s)^2 + y^2}{x^2 + y^2}\right]^{1/2} \quad (11)$$

$$v_s = \frac{q_j}{2\pi}\tan^{-1}\left(\frac{sy}{x^2 - sx + y^2}\right) \quad (12)$$

The strengths of the q_j on the surface of the ejector shroud are determined by simultaneously satisfying the known entrainment (inflow) boundary condition due to the wall jet on the inner surface of the shroud, and the condition of zero flow through the outer surface. The solution yields sinks (negative sources) on the inner surface and positive sources on the outer surface.

76

INVISCID, OUTER SOLUTION

The circulation generated around each section of the ejector shroud is calculated by solving a system of equations which specify that the shroud must be a streamline of the flow induced by the entrainment of the jets. A vortex lattice method was used to determine the circulation density. The continuous vorticity distribution is replaced by n discrete vortices of strength Γ_j, located at x_j, the quarter chord of the panels shown in Figure 2. It was found that better results were obtained if the vortex sheet is placed on the inner surface of the shroud, rather than on the mean camber line. All the flow singularities which represent the shroud geometry and jet effects must induce the known entrainment (inflow) velocities on the surface of the shroud. However, the source/sink distribution on each surface already satisfies this boundary condition. Therefore, the resultant of the velocities induced by all the other singularities must be tangent to the inner surface of the shroud; that is, the normal velocity induced by the vortex sheet must be equal but opposite to the normal velocity induced by the central jet and opposite wall jet.

The vortex strengths are determined by satisfying this boundary condition at n points which correspond to the three quarter chord station on each panel. The horizontal and vertical components of velocity induced at a point $P(x_i, y_i)$ by the vortex pair of strength Γ_j at the points $P(x_j, y_j)$ and $P(x_j, -y_j)$ are

$$u(x_i, y_i) = \left(\frac{y_j - y_i}{2\pi r_{ij}^2} - \frac{y_j + y_i}{2\pi r_{i,-j}^2} \right) \Gamma_j \qquad (13)$$

$$v(x_i, y_i) = \left(\frac{x_j - x_i}{2\pi r_{ij}^2} + \frac{x_j - x_i}{2\pi r_{i,-j}^2} \right) \Gamma_j \qquad (14)$$

in which $r_{ij} = \left[(x_i - x_j)^2 + (y_i - y_j)^2 \right]^{1/2}$ is the distance between points. Thus, the contribution to the velocity normal to panel-i by both vortex sheets is

$$U_v = \sum_j (b_{ij} \cos \alpha_i - a_{ij} \sin \alpha_i) \, \Gamma_j \qquad (15)$$

in which the influence coefficients, a_{ij} and b_{ij}, have the form given in Equations (13) and (14), and α_i is the angle of panel-i relative to the ejector axis. Similarly, the normal velocity induced by the central jet and the opposite wall jet is

$$U_S = \sum_j (d_{ij} \cos \alpha_i - c_{ij} \sin \alpha_i) \, q_j \qquad (16)$$

in which the range of the index j is over both jets. Since the resultant
of the normal velocities induced by the jet and vortex sheet must be zero,
U_v is set equal but opposite to U_s at each control point. The resulting set
of simultaneous equations is solved for the Γ_j by triangularization of the
coefficient matrix.

SOLUTION MATCHING PROCEDURE

Method of Iteration

The inner and outer routines are incorporated into a single computer program
which yields a matched solution by iterating between the rate of entrainment
by the jets and the circulation around the shroud. The circulation determines
the sink strengths by controlling the secondary velocity at the ejector inlet.
Conversely, the sink distribution determines the circulation by controlling
the velocity field in which the shroud "flies." A unique matched solution is
established by satisfying the appropriate Kutta condition, which depends on
the exhaust jet momentum, as follows.

When the ejector is short or the diffuser angle is large, curvature of the
jet sheet leaving the trailing edge supports a low pressure region behind
the ejector, as shown in Figure 3. Morel and Lissaman[8] noted that the effect
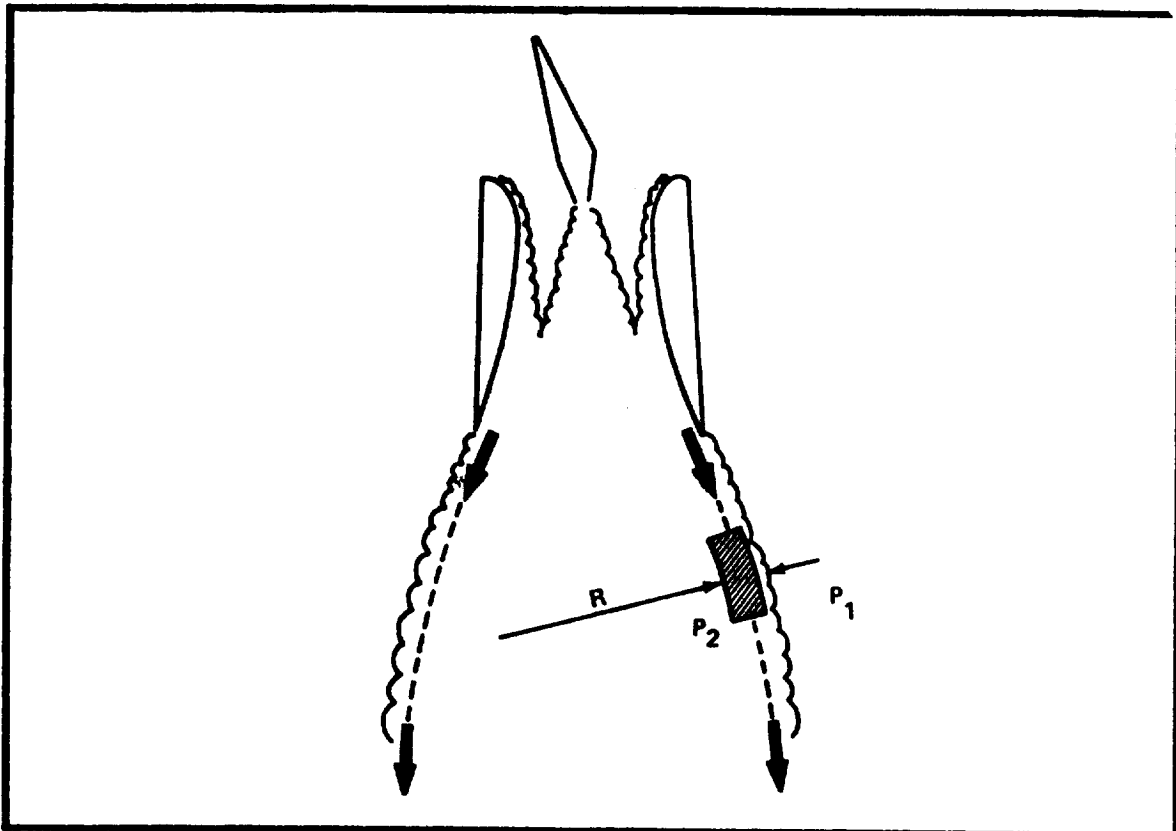

Figure 3. Curvature of the Trailing Jet Balances the Pressure Difference.

is similar to that of a jet flap and described the phenomenon as a "jet flap diffuser." The influence of the jet flap is calculated using an approach suggested by the classical jet flap theory of Spence.[9] Since the pressure difference is balanced by inertia forces due to curvature of the jet sheet, the radius of jet curvature, R, is given by

$$\frac{T}{R} = \Delta P \qquad (17)$$

in which T is the thrust of the wall jet at the ejector exit. To a first approximation, both the jet thrust and radius of curvature can be assumed constant. The pressure difference across the trailing jet sheet is related to the strength of an equivalent vortex sheet,

$$\rho u \gamma = \Delta P \qquad (18)$$

so that the basic mathematical problem becomes finding a vorticity distribution which makes the jet sheet a streamline of the flow.

These two additional boundary conditions for the shape and strength of the jet flap diffuser are satisfied as part of the iteration to match the inner and outer solutions. When the iteration converges and the solutions are matched, the pressure within the ejector reaches atmospheric pressure at the point where the jet sheets become parallel to each other and the axis of the ejector. In effect, the Kutta condition for the vorticity distribution is satisfied at the end of the jet flap diffuser, rather than at the trailing edge of the ejector shroud.

Evaluation of the Thrust Augmentation

The thrust of the ejector is evaluated by integrating the thrust of the mixed flow at the ejector exit. It is given by

$$\tau = \int_{Ae} u^2 dy - (P_a - P_e)A_e \qquad (19)$$

in which P_e and A_e are the static pressure and area at the exit. Because the flow velocities are constant over a small control volume surrounding each grid point, integration of the stream thrust involves a simple summation of the thrust increment from each control volume. The static pressure is constant across the exit. It should be noted that even though the pressure force is negative, lowering the exhaust pressure, as with the jet flap diffuser, results in a net thrust increase. This is because the momentum flux is increased more than the pressure force is reduced.

In order to evaluate the basic lifting surface theory that the force on the shroud is related to the lift on a wing, the prediction of this analysis will be compared to experimental data. A sketch of the test ejector is shown in Figure 4. It combines a single central nozzle with Coanda jets on the
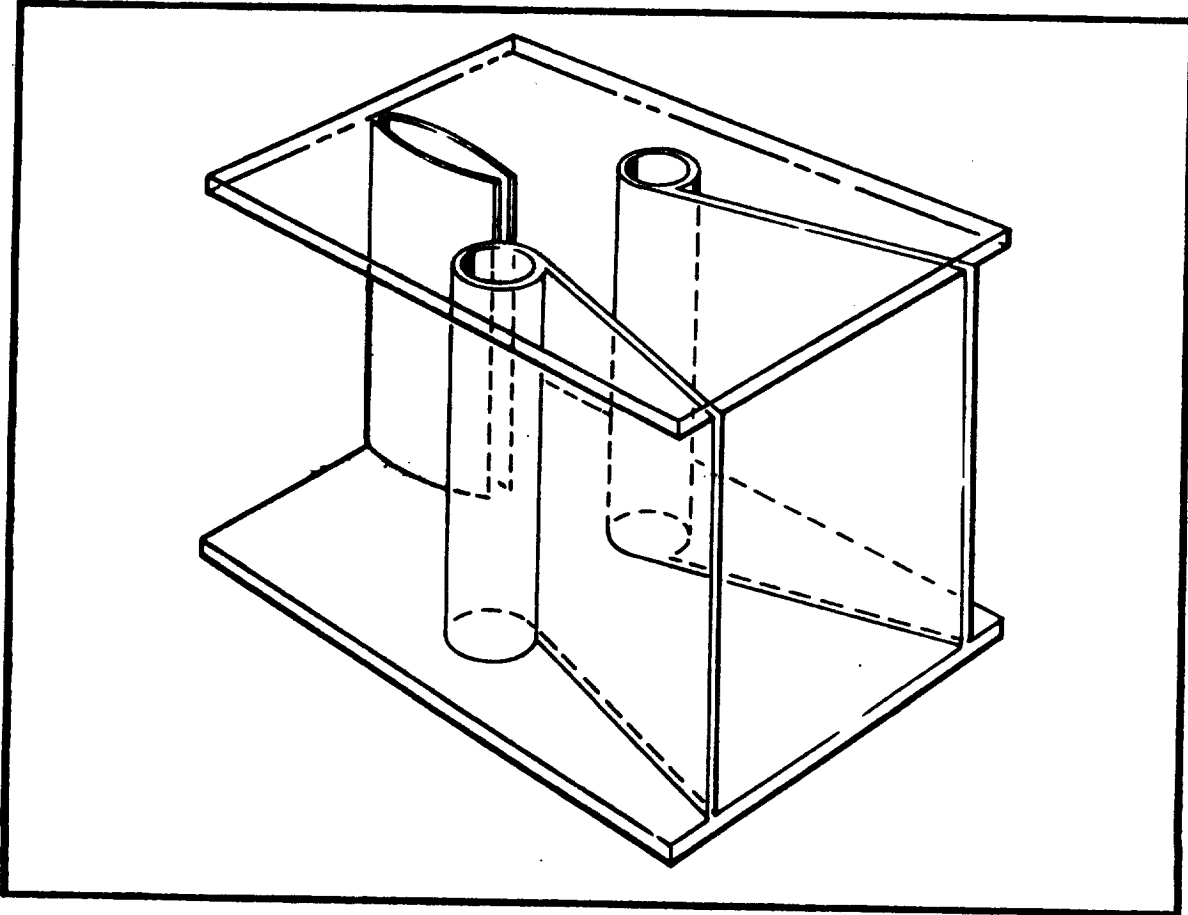

Figure 4. Sketch of the Experimental Ejector.

inner surface of the shroud. A slot in each endwall at the ejector throat provides a boundary layer control jet to prevent separation of the flow from these surfaces. In this configuration 60% of the primary flow is in the central jet, 17% goes to each of the Coanda jets, and the remaining 6% of the primary flow is divided between the two endwall jets. The ejector has a span of 36 cm, a length of 27 cm, and has a throat 12 cm wide. The inlet area ratio is approximately 11.

The calculated jet boundaries are compared with the measured boundaries in Figure 5. Since the turbulence constants were not adjusted for this case, but derived from other flows, the agreement is particularly good. The predictions of the shape and length of the jet flap diffuser are also satisfactory. In Figure 6 the calculated velocity distributions at three stations within the
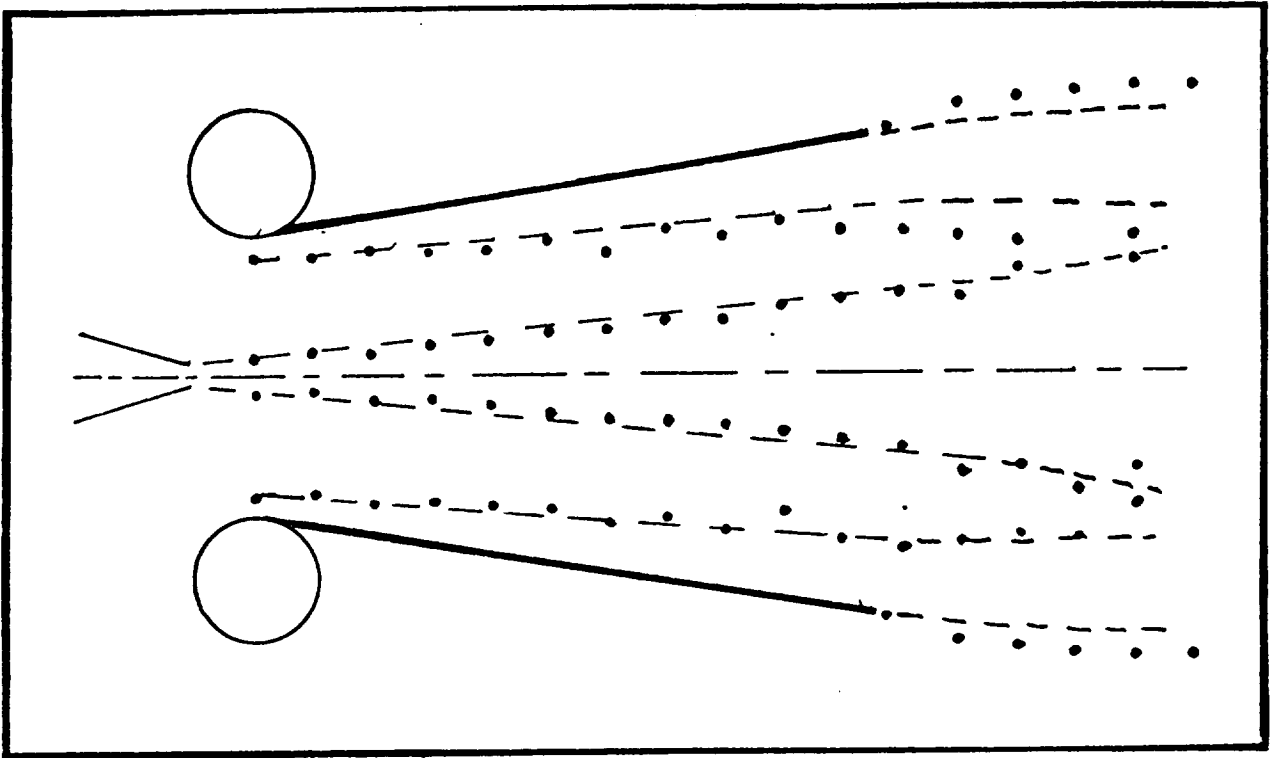
80

Figure 5. Comparison of Calculated (--) and Measured (●) Jet Spreading Rates.
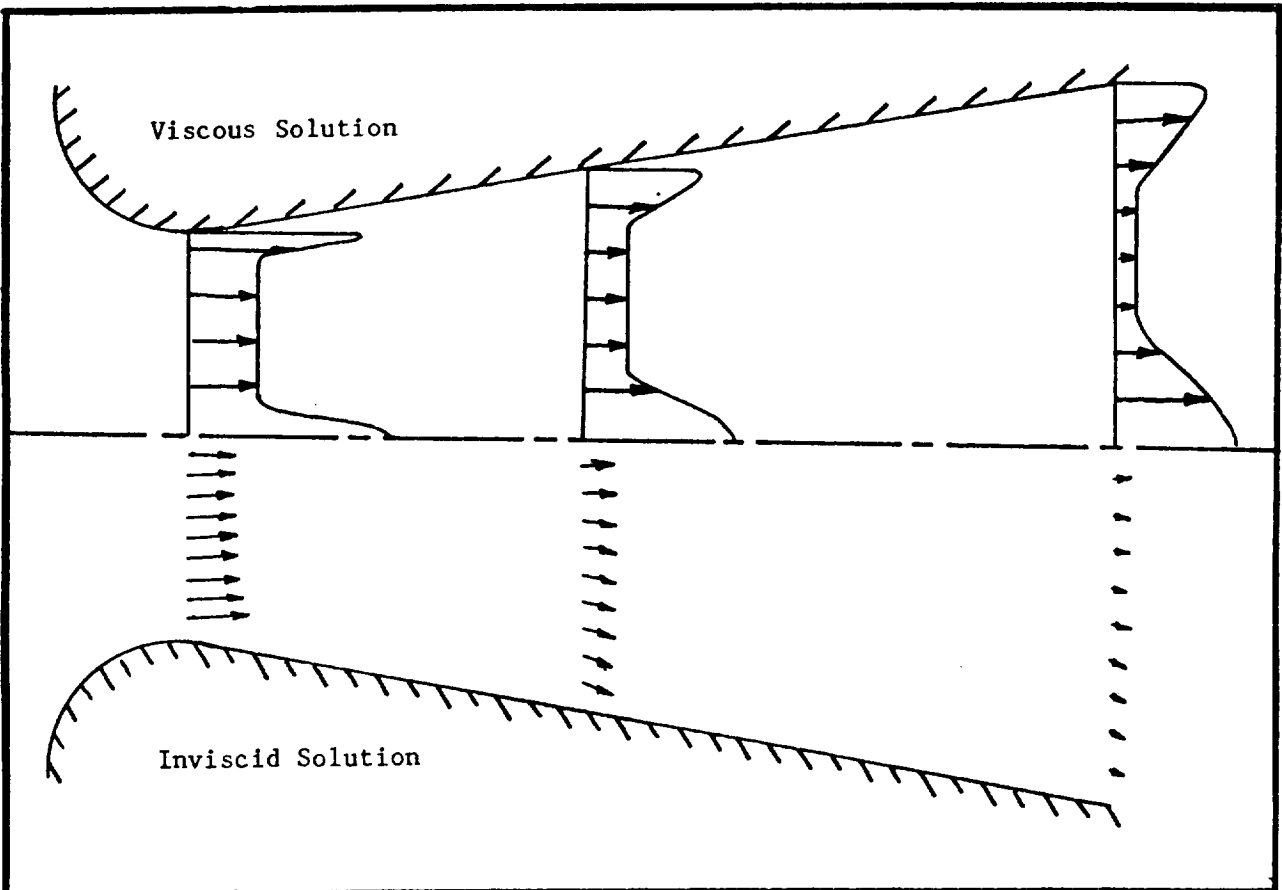
Viscous Solution

Inviscid Solution

Figure 6. Comparison of Velocity Distributions Calculated by Viscous and Inviscid Solutions.

ejector are compared. The profiles from the inner, viscous solution show the spreading of the jets, as well as the reduction in secondary velocities. Due to the assumption that the static pressures are constant at each axial station, the secondary velocities in the viscous solution are uniform; further, there is no transverse velocity component. The inviscid velocity distributions, shown on the other side of the ejector, indicate the extent of the actual skewness and the magnitude of the transverse velocities. Since the jets are replaced by equivalent sinks in the inviscid solution, The jet profiles are not seen in this case.

In Figure 7 the calculated change in the thrust augmentation ratio with the diffuser area ratio is compared to experimental values. At low diffuser area
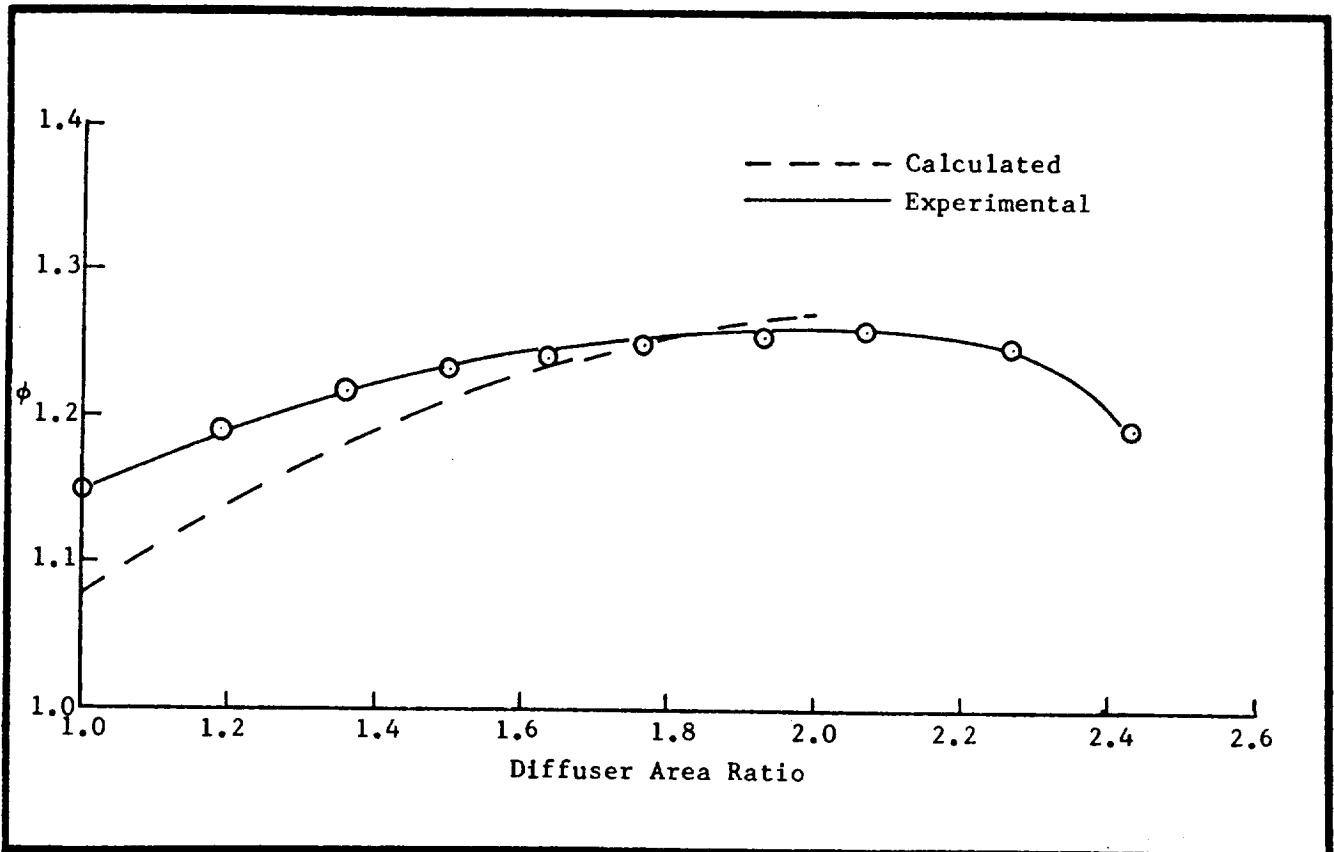

Figure 7. Comparison of the Effect of Calculated and Experimental Changes in the Diffuser Area Ratio.

ratios the thrust augmentation is underpredicted by approximately 6%, while good predictions of the maximum augmentation are obtained. This result is a consequence of the approach taken in calculating the jet flap effect. Because the length of the jet flap diffuser is defined by the point where

the jet sheets becomes parallel, the jet diffuser length goes to zero as the diffuser angle of the duct is reduced. Most of the discrepancy at the low diffuser area ratios can probably be attributed to this effect. With this perspective, the agreement between analysis and experiment can be judged satisfactory.

Figure 8 shows the predicted variation of the thrust augmentation ratio as a function of inlet area ratio, for a constant diffuser area ratio of 1.8.
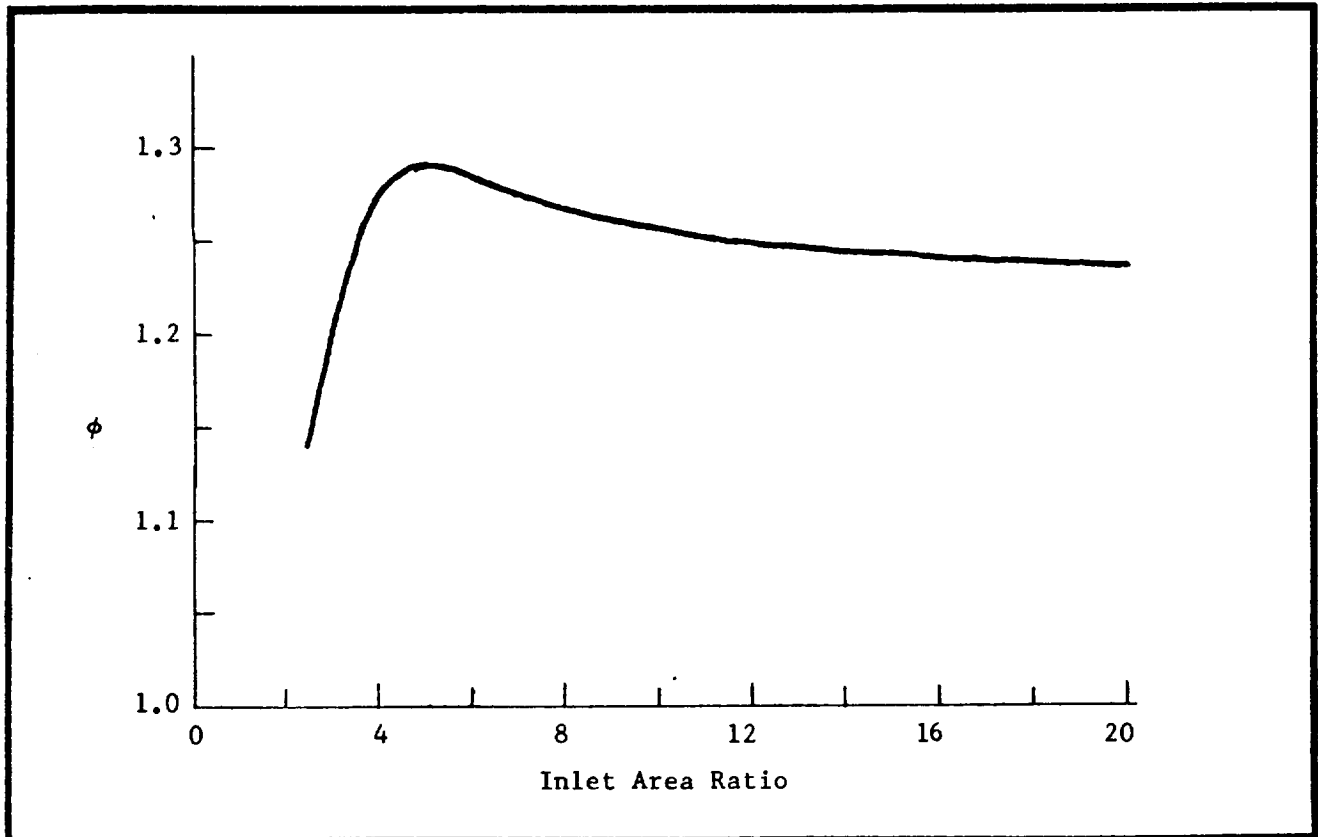

Figure 8. Predicted Effect of Inlet Area Ratio.

The length of the shroud was kept constant, so that the ejector becomes relatively long at low inlet area ratios. In this case the parabolic flow approximation is valid, and the augmentation is seen to initially increase with the inlet area ratio. This is as predicted by the momentum theories. As the sides of the shroud are moved further apart, the strength and influence of the circulation is diminished, and the augmentation begins to decrease. This is according to the lifting surface theory. Thus, the correct behavior has been predicted in each limit.

CONCLUSIONS

A viscous/inviscid interaction analysis has been used to extend classical momentum theories of ejector thrust augmentation. The primary elliptic effects have been included by iterating between a parabolic solution for the flow through the ejector and an elliptic solution for the flow outside the ejector. Briefly, a calculation of the rate of entrainment by the turbulent jets is used to determine the equivalent sink strengths. The requirement that the ejector shroud must be a streamline of the flow induced by these sinks is then used to evaluate the circulation generated around the shroud. The influence of the circulation is included in the next iteration for the rate of entrainment. Comparison of the calculated thrust augmentation with experimental data establishes confidence in the ability to predict the complex ejector flowfield with this approach. In addition, greater understanding of the principle of ejector thrust augmentation is obtained from the analysis.

REFERENCES

1. von Karman, T., "Theoretical Remarks on Thrust Augmentation," in Contributions to Applied Mechanics, Reissner Anniversary Volume, pub. by J. W. Edwards, Ann Arbor, Michigan, 1949, pp 461-468.

2. Gilbert, G. B. and Hill, P. G., "Analysis and Testing of Two-Dimensional Slot Nozzle Ejectors with Variable Area Mixing Sections," NASA CR-2251, 1973.

3. DeJoode, A. D. and Patankar, S. V., "Prediction of Three-Dimensional Turbulent Mixing in an Ejector," AIAA Journal, Vol. 16, No. 2, February 1978, pp 145-150.

4. Bevilaqua, P. M., "Evaluation of Hypermixing for Thrust Augmenting Ejectors," Journal of Aircraft, Vol. 11, No. 6, June 1974, pp 348-354.

5. Bevilaqua, P. M., "Lifting Surface Theory for Thrust Augmenting Ejectors," AIAA Journal, Vol. 16, No. 5, May 1978, pp 475-481.

6. Launder, B. E. and Spalding, D. B., "The Numerical Computation of Turbulent Flows," Computer Methods in Appl. Mech. and Eng., Vol. 3, No. 2, March 1974, pp 269-289.

7. Patankar, S. V. and Spalding, D. B., "Heat and Mass Transfer in Boundary Layers," International Textbook Company, Ltd, London, 1970.

8. Morel, J. P. and Lissaman, B. S., "The Jet Flap Diffuser, a New Thrust Augmenting Device," AIAA Paper No. 69-777, 1969.

9. Spence, D. A., "The Lift Coefficient of a Thin, Jet-Flapped Wing," Royal Society of London, Proceedings, Vol. 238, Jan. 1957, pp 46-68.